Iran J Pharm Res. 2022 December; 21(1):e127486. doi: 10.5812/ijpr-127486.

Published online 2022 August 20. **Research Article**

# Ocular Delivery of Quercetin Using Microemulsion System: Design, Characterization, and Ex-vivo Transcorneal Permeation

Eskandar Moghimipour [1, 2], Negar Farsimadan [2] and Anayatollah Salimi [1, 2, *]

[1] Nanotechnology Research Center, Ahvaz Jundishapur University of Medical Sciences, Ahvaz, Iran

[2] Department of Pharmaceutics, School of Pharmacy, Ahvaz Jundishapur University of Medical Sciences, Ahvaz, Iran

[*] *Corresponding author*: Department of Pharmaceutics, School of Pharmacy, Ahvaz Jundishapur University of Medical Sciences, Ahvaz, Iran. Email: anayatsalimi2003@yahoo.com

**Received** 2022 May 17; **Revised** 2022 June 21; **Accepted** 2022 July 19.

## Abstract

**Background:** The goal of this research was to design and characterize quercetin microemulsions (MEs) to resolve water solubility issues related to quercetin and improve transcorneal permeation into the eye.

**Methods:** MEs were prepared by the phase diagram method. Oily phase (oleic acid-Transcutol P), surfactant (Tween 80, Span 20), and co-surfactant (propylene glycol) were used to make a quercetin-loaded ME. The size of the droplets, their viscosity, pH, release, flux, and diffusivity were all measured.

**Results:** Droplet diameters in ME samples ranged from 5.31 to 26.07 nanometers. The pH varied from 5.22 to 6.20, and the release test revealed that 98.06 percent of the medication was released during the first 24 hours. The flux and diffusivity coefficients of the ME-QU-8 formulation were 58.8 $\mu g/cm^2.h$ and 0.009 $cm^2/h$, respectively, which were 8.8 and 17.9 times greater than the quercetin aqueous control (0.2 percent). The maximum percentage of drug permeated through rabbit cornea after five hours was 16.11%.

**Conclusions:** It is concluded that ME containing quercetin could increase transcorneal permeation and that permeation could be altered by any change in the composition of the ME formulation. This effect might be caused by structural alterations in the cornea caused by ME components.

*Keywords:* Corneal, Permeability, Microemulsion, Quercetin, Rabbit, Release

## 1. Background

The ocular drug delivery route is of great interest because of the physiological and physicochemical structures found within the eye. Owing to such structures, eyes tend to resist the permeation of drugs, meaning that certain substances must be administered to the eye (and retained by the eye) to ensure effective treatment. Eye drops represent the most common ocular drug administration method. This method's most significant drawback is eye drops' low bioavailability—roughly 70% of the administered drug does not reach its target (1). Various anatomical and physiological barriers—for example, nasolacrimal drainage, the drug's inadequate time spent in the precorneal area, and low corneal permeability—represent the primary reasons for drugs' poor bioavailability when delivered ocularly (2).

The cornea's main purpose is protecting intraocular tissues. The membrane of the cornea comprises several layers each with unique characteristics. These layers include the epithelium, stroma, and endothelium, with the first two playing significant roles in drug absorption. It is not possible for drugs with high hydrophilic or lipophilic effects to pass through the cornea via passive transport, as the stroma and epithelium are membranes that have rate-limiting role for permeation of hydrophobic and hydrophilic compouds, respectively (3-5). The impenetrability of the corneal epithelium layer and associated short retention time of drugs mean that drugs administered as eye drops have poor corneal permeability. Because of these challenges, ocular nanocarriers (e.g., solid lipid nanoparticles, micelles, liposomes, and microemulsions) are used to improve ocular drug delivery (6-9).

Quercetin is a natural flavonoid with low toxicity when administered orally or intravenously that has received significant attention from researchers owing to its anticancer, anti-inflammation, and antioxidant effects (10-13). Moreover, quercetin might help reduce the oxidative stress associated with eye complications including senile cataracts, (14) as well as age-related macular degeneration (ADME) which causes retinal epithelium damage. Quercetin also promotes ROS-catalyzing protein ex-

pression, and therefore, might also help protect the eyes against pro-inflammatory factor (IL-6) synthesis (15). According to murine uveitis models, this anti-inflammatory potential is related to quercetin's ability to suppress retinal S antigen-induced intraocular inflammation (16). Of note, quercetin cannot be taken orally as this delivery method results in poor bioavailability and permeability, as well as considerable first-pass metabolism (12).

MEs are liquid mixtures consisting of oil, water, and surfactants, and they are transparent, thermodynamically stable, and isotropic. They range from 10-100 nm in size and exhibit minimal surface tension. The properties of MEs are ideal for helping drugs pass through the cornea, thus making them advantageous carriers during ocular drug delivery (17-19). Moreover, ME carriers contain surfactants and co-surfactants, which also assist in corneal drug penetration. Furthermore, MEs' low surface tension allows them to spread easily across the cornea; this further assists drug delivery by increasing the area of the corneal epithelial surface that the drug reaches. ME holds significant promise for topical ophthalmic application due to their eye-drop-like consistency, nano droplet size range, and phase transition behavior (20).

## 2. Objectives

The remainder of this paper explains how ME carriers were designed to aid the ocular delivery of quercetin. In addition, it was investigated whether the percentage of the drug that permeated rabbit corneas could be increased.

## 3. Methods

### 3.1. Materials

The Solarbio Company supplied the quercetin (China). Merck provided the rest of the needed components, such as span 20, tween 80, and oleic acid (Germany). The diethylene glycol monoethyl ether (Transcutol P) used in this investigation was given by the GATTEFOSSE Company (France).

### 3.2. Animals

The rabbits used in this investigation were male New Zealand white rabbits weighing 2.5 - 3.5 kg. The current experiment was approved by the Ahvaz Jundishapur University of Medical Sciences' animal ethics committee (permission number IR.AJUMS.ABHC.REC.1397.020).

### 3.3. Quercetin Solubility

Quercetin's solubility in oily phase (i.e., Transcutol P, oleic acid), surfactant phase (Span 20, Tween 80), and a co-surfactant (propylene glycol) was examined. First, several excess samples of quercetin were taken and dissolved in each of the aforementioned substances (5 mL for each substance) and stirred for 48 hours at 37°C (6). Afterward, centrifugation (3000 rpm for 15 minutes) was performed for all samples. This process eliminated any undissolved portion of the drug from the solution. The next step involved filtering the clear supernatants and then using UV spectrophotometry to assess them (21).

### 3.4. Phase Diagram Construction

The ranges of the concentrations of different ingredients for the existing boundary of MEs were examined based on phase diagrams of free drug MEs. This process was carried out by constructing two-phase diagrams with two different weight ratios (1:1 and 3:1) of Tween80/Span 20-propylene glycol. For each phase diagram, the surfactant mixture was added to the oleic acid/Transcutol P (10:1) blend at varied weight ratios (i.e., 1:9, 2:8, 3:7, 4:6, 5:5, 6:4, 7:3, 8:2, and 9:1). During this step, a magnetic stirrer was employed to mix all solutions. Once sufficiently mixed, each mixture was diluted into double distilled water using a dropper at $25 \pm 1$°C. Once a mixture became a clear liquid, it was considered a ME (22).

### 3.5. Polarized Light Microscopy

Cross-polarized light microscopy (Olympus BX53 P, Tokyo, Japan) was utilized to check whether all samples possessed the isotropic property of MEs. This was accomplished by observing a drop of each sample under a cross-polarized light after putting it between a coverslip and a glass slide. Whereas anisotropic liquid crystals interfere with the polarized light, isotropic substances do not—therefore, if the field did not become brighter during this step, the sample was confirmed as being a ME (22).

### 3.6. Preparation of Microemulsions

The boundaries of the MEs were determined using the phase diagrams. Thereafter, three variables, each at two levels (resulting in a total of eight ME formulations), were implemented not a full factorial design. Surfactant/co-surfactant ratio (S/C), as well as the oil and water percentages (%oil and %W), were the primary variables used to determine each ME's qualities. Each of the eight ME formulations had either low (5%) or high (50%) oil content, low (5%) or high (10%) water content, and a low (1:1) or high (3:1) S/Co mixing ratio.

MEs with Tween 80/Span 20-propylene glycol weight ratios of either 1:1 or 3:1 were selected from the phase diagram (Table 1). The oil phase of each ME had quercetin (0.2%) added to it, followed by the (dropwise) addition of an S/Co mixture and double distilled water. Finally, each mixture was stirred at ambient temperature until becoming a clear liquid (23, 24).

**Table 1.** The Solubility of Quercetin in Different Oils, Surfactants and Co-surfactants (n = 3)

| Phase | Excipient | Solubility (mg/mL), Mean ± SD |
|---|---|---|
| **Oil** | Transcutol p (Tp) | 285.2 ± 5.2 |
| **Oil** | Oleic acid | 0.15 ± 0.01 |
| **Oil** | Oleic acid-Tp | 278.1 ± 6.1 |
| **Surfactant** | Tween80 | 37 ± 0.32 |
| **Surfactant** | Span20 | 0.712 ± 0.001 |
| **Co-surfactant** | Propylene glycol | 0.819 ± 0.1 |
| **Water** | Water | 0.000171 ± 0.000027 |

### 3.7. Droplet Size

The MEs' droplet size ranges were determined by a SCATTER SCOPE 1 QUIDIX apparatus (operated at 250C).

### 3.8. Viscosity

A Brookfield viscometer apparatus (DV-II + Pro Brookfield, USA) (spindle no. 34; shear rate = 50 rpm) was used to obtain all MEs' viscosities (25).

### 3.9. Surface Tension

A tensiometer apparatus was utilized to calculate the surface tension of MEs at 25 ± 0.5°C.

### 3.10. Physical Stability Experiments

Thermal stability and centrifuge strain tests were carried out to evaluate each ME's physical stability. Afterward, following the protocol provided by the ICH, the samples were kept at various temperatures (4°C, 25°C, 37°C, and 75% ± 5% RH) for six months before being reassessed. These reassessments were performed to examine whether the physicochemical properties (e.g., phase separation, droplet size) of the MEs varied depending on the time elapsed and the temperature at which they were stored. As part of this step, all MEs were centrifuged at 25°C for 30 minutes at 15,000 rpm (26).

### 3.11. In Vitro Drug Release

The release rate of quercetin from each ME was measured using Franz diffusion cells that having a contact area of 0.348 $cm^2$ and a cellulose membrane was placed between the donor and receptor chambers. The next step, 0.5 mL of quercetin MEs were transferred to the membrane. Then, 10 mL of buffer phosphate (pH = 7.4) and a methanol solution (4:1) were added to each receptor medium. Furthermore, all receptor media were stirred constantly at 100 rpm by externally driven magnetic beads.

Then, a 1-mL sample of each solution was extracted from each receptor compartment; sink conditions were maintained by immediately adding 1 mL of a fresh receptor medium to the compartment after the sample was extracted. This was done several times for each compartment at predetermined time intervals (0.5, 1, 2, 3, 4, 5, 6, 7, 8, and 24 hours). After the samples were extracted, a UV spectrophotometer (at 382 nm) was employed to evaluate all samples. The next step involved plotting the drug release percentages for each time interval and examining each sample's behavior. This was done by fitting each sample onto various kinetic models (e.g., zero, first, and Higuchi models) (27).

### 3.12. Differential Scanning Calorimetry

A Mettler Toledo Differential Scanning Calorimetry (DSC) apparatus was employed to determine the DSC of each sample. The apparatus was equipped with a refrigerated cooling system that provided a minimum temperature of -45°C). Aluminum pans had roughly 6 - 11 mg of each ME added to them and were then sealed immediately to prevent water evaporation. At the same time, an empty pan (as a reference) served as a reference condition. The pan was kept at temperatures of -50 - 30°C at a scan rate of 5°C/min. The endothermic and exothermic peaks of the DSC thermograms were considered when recording the changes in enthalpy amounts ($\Delta H$) (27).

### 3.13. Ex-vivo Corneal Permeability

The intact subcutaneous tissues of eye corneas (with sclera rings) of male New Zealand Albino rabbits were removed using scissors and a scalpel. The corneal epithelium needed to be preserved, and so they were stored in a chondroitin-sulphate-based commercial storage media called DexSol (Chiron Ophthalmic, Irvine, California) (28, 29).

Modified Franz diffusion cells were utilized to carry out all ex vivo corneal permeability experiments. These cells were produced in the lab and had an effective diffusion area of 0.348 $cm^2$. The excised corneas were placed between each cell's donor and receptor chambers. In this way, the sclera ring of each cornea was fixed between these two

compartments. This orientation also protected the cornea from any damage that the diffusion cell apparatus might cause.

A buffer phosphate solution (pH = 7.4) and methanol (4:1) were added to each receptor chamber. This solution was thermostated at 32 ± 0.5°C and stirred at 200 rpm rate using magnets during the experiment. After being carefully measured, all quercetin ME samples (0.5 mL) were added to the corneal surfaces. Non-occlusive conditions were applied to the experiments, as such conditions allow air to permeate the corneal tissues. Then, UV spectrophotometric analysis (at 382 nm) began by taking a 1-mL sample from each receptor medium. Sink conditions were maintained by immediately adding 1 mL of a fresh receptor medium after the sample was extracted. This was done several times at set intervals of 0.5, 1, 2, 3, 4, and 5 hours. This process also included blanks (i.e., drug-free MEs). This test was replicated for the quercetin suspension (0.2%), and comparisons were made in terms of drug permeation. The results were represented based on what percentage of the drug permeated at different times (30, 31).

### 3.14. Data Analysis and Statistics

Quercetin permeation in each unit of the cornea area was measured and recorded as a function of time. Various parameters related to corneal permeability were considered based on previous studies on corneal permeation. Flux ($J_{ss}$), permeability coefficient (P), lag time (Tlag), and diffusivity coefficient (D) were the metrics in question.

The linear part of the permeability curve slope was utilized to attain the flux ($J_{ss}$, $\mu g/cm^2h$). Appearance D ($D_{app}$) is used to define the diffusivity coefficient, as the cornea thickness (h) contains no direct drug permeation pathway for. Furthermore, the equation $P_{app}= J_{ess}/C_0$ was used to calculate the apparent permeability coefficient ($P_{app}$, cm/h); meanwhile, $D_{app} = h^2/6\ T_{lag}$ was used to find the apparent diffusivity coefficient ($D_{app}$ $cm^2/h$).

The linear part of the permeability curve was extrapolated to the time axis to attain the $T_{lag}$ value (in hours). Data (recorded as mean ± SD) were recorded after repeating the experiments three times.

### 3.15. Effect of Quercetin ME on the Cornea Structure

Increased tissue corneal hydration-induced cornea changes via drug formulation were assessed using different methods such as DSC. Experiments were done using a Mettler Toledo DSC. Prepared corneas were immersed in a quercetin ME formulation for 5 hours. Then, any excess amount of quercetin ME formulation was removed and sealed in an aluminum pan. The thermograms were recorded within a range of 30 to 200°C (scan rate = 10°C/min). Results are presented as the effect of quercetin ME formulation on transition temperature and the enthalpy of the transition phase (32).

## 4. Results and Discussion

### 4.1. Solubility of Quercetin

Table 1 provides the quercetin solubility data for all ME samples. In this study, oleic acid was employed, as its compatibility with Tween 80 makes it an appropriate oil phase for the experiments that were carried out. Quercetin exhibits moderate solubility when introduced to this oil phase (0.15 ± 0.01 mg/mL). Nevertheless, previous investigations show that Tween 80 creates a homogenized interface by interfering with oleic acid's drop surface, thus preventing the aggregatin of droplets (20). Oleic acid is a monounsaturated fatty acid group that plays a significant role in the formation of MEs and is frequently used as the oily phase of ophthalmic MEs. The selection of the surfactant phase is a very essential step in the design of an ME system. When MEs are prepared, surfactant molecules are adsorbed by water in the oil interface and form initial curvature around the internal phase in MEs. The addition of a cosurfactant (propylene glycol) helps to complete the curvature of the surfactant film. The penetration of cosurfactant into the interfacial film produces a more fluid interface by allowing the hydrophobic tails of the surfactants to move freely at the interface. Generally, low-molecular-weight alcohols and glycols with chain length ranging from $C_2$ to $C_{10}$ are used as cosurfactants in preparing stable ME. Propylene glycol has two important roles in ocular MEs. The first role is as a cosurfactant to improve the physical stability and prevent phase separation of the ME. The second role is to add a demulcent effect to ocular ME in order to relieve any irritant effect that may result from the presence of surfactants. Other suitable properties for nonionic surfactants are the absence (or very low amounts) of ophthalmic toxicity. Among the different groups of surfactants, nonionic surfactants are most often used for this purpose owing to their favorable solubilization, enhanced permeability, and nonirritant effects. Tween 80, Span 20 (as a surfactant), and propylene glycol (as a co-surfactant) are commonly used in ophthalmic MEs (23).

### 4.2. Phase Diagram Studies

The phase diagrams of oleic acid-Transcutol P (10:1)/Tween 80 Span 20/propylene glycol/water are shown in Figure 1. In this diagrams, we show that by increasing the surfactant/co-surfactant ratio (Km) from 3:1 to 1:1, the zones of ME were increased. In addition, our results indicate that by increasing the co-surfactant amounts, ME zones were decreased.

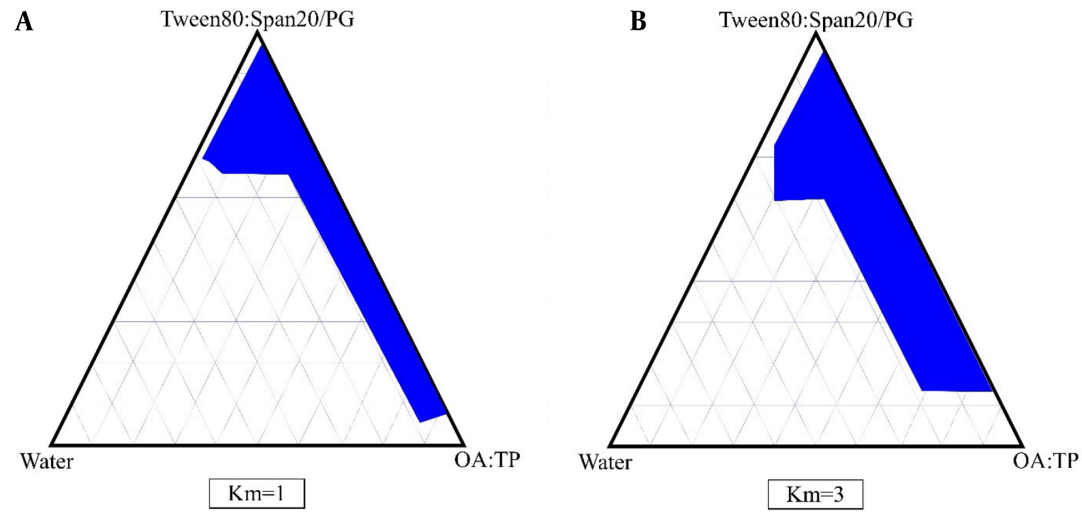


**Figure 1.** The pseudo ternary phase diagrams of the oil-surfactant/co-surfactant mixture-water system at 1:1 (A) and 3:1 (B) weight ratios of Tween 80/Span 20/PG at ambient temperature; dark area shows microemulsions boundary.

**Table 2.** The Composition of Quercetin Microemulsion Formulations and pH, Viscosity, Droplet Size (in the Beginning and 6 Months After Experiment), Surface Tension, and Polydispersity Index of Quercetin Microemulsions

| Formulation | State in Full Factorial Design | (S:C) | %Oil | %S + C | %Water | %Quercetin | pH | Viscosity (cps) | Droplet Size (nm) | Mean Droplet Size After 6 Month (nm) | Surface Tension, dyne/cm | Polydispersity Index |
|---|---|---|---|---|---|---|---|---|---|---|---|---|
| ME-QU-1 | +++ | 3 | 50 | 40 | 10 | 0.2 | 5.22 ± 0.02 | 142 ± 1.1 | 10.33 ± 0.10 | 10.4 ± 0.7 | 34.3 ± 0.8 | 0.41 ± 0.02 |
| ME-QU-2 | ++- | 3 | 50 | 45 | 5 | 0.2 | 5.24 ± 0.02 | 135 ± 1.3 | 5.31 ± 0.99 | 5.6 ± 0.8 | 34.5 ± 0.1 | 0.375 ± 0.01 |
| ME-QU-3 | +-+ | 3 | 5 | 85 | 10 | 0.2 | 5.31 ± 0.01 | 325 ± 1.5 | 9.04 ± 0.8 | 9.2 ± 0.7 | 34.7 ± 0.8 | 0.36 ± 0.02 |
| ME-QU-4 | +-- | 3 | 5 | 90 | 5 | 0.2 | 5.34 ± 0.02 | 361 ± 1.4 | 9.04 ± 0.75 | 9.3 ± 0.1 | 35.2 ± 0.6 | 0.348 ± 0.01 |
| ME-QU-5 | -+ | 1 | 5 | 85 | 10 | 0.2 | 5.42 ± 0.02 | 210 ± 1.3 | 9.52 ± 0.3 | 9.8 ± 0.2 | 32.9 ± 0.1 | 0.375 ± 0.001 |
| ME-QU-6 | -- | 1 | 5 | 90 | 5 | 0.2 | 5.93 ± 0.02 | 225 ± 1.5 | 26.07 ± 0.7 | 26.5 ± 0.3 | 33.6 ± 0.1 | 0.380 ± 0.007 |
| ME-QU-7 | -+- | 1 | 50 | 45 | 5 | 0.2 | 6.14 ± 0.02 | 120 ± 0.98 | 5.7 ± 0.5 | 6.01 ± 0.1 | 19.2 ± 0.4 | 0.380 ± 0.007 |
| ME-QU-8 | -++ | 1 | 50 | 40 | 10 | 0.2 | 6.20 ± 0.02 | 115 ± 0.78 | 8.85 ± 0.76 | 9.1 ± 0.2 | 21.7 ± 0.2 | 0.380 ± 0.008 |

### 4.3. Polarized Light Microscopy

Isotropic substances, such as MEs, do not interfere with polarized light and have a black field of vision (unlike anisotropic liquid crystals). Under polarized light microscopy.

### 4.4. Characterization of the Quercetin Microemulsions

We chose eight distinct ME compositions from the phase diagrams with Tween 80-Span 20/PG weight ratios of 1:1 and 3:1 to examine the functions of varied composition quantities in the ME structures and their impacts on features and ocular penetration. The components of selected ME formulations are shown in Table 2.

Table 2 provides data related to the quercetin MEs'viscosity, surface tension, polydispersity index (PI), mean droplet size, and pH. As shown in the table, the average viscosity of the examined ME samples ranged from 115 - 361 cps. Meanwhile, the average pH was 5.22 - 6.20, and the average droplet size was 5.31 - 26.07 nm, with all droplets less than 30 nm in size. It was also found that the particle size decreased as surface area increased, which, in turn, caused bioavailability to increase. An analysis of the PI values revealed that the particle sizes of the MEs were similar, as no PI value exceeded 0.41. Similarly, the droplets of all quercetin ME samples were of a similar size (33). According to statistical data, particle size was not significantly related to any of the independent variables ($P > 0.05$) based on particle size measurements. The particle sizes of ME-QU-6 and ME-QU-2 are the greatest and smallest, respectively. Statistical results also revealed that the correlation between the mean pH and the independent variable (S/C ratio) was significant ($P < 0.05$). This finding indicates that pH increases as the S/C ratio decreases. Moreover, statistical results indicate that viscosity's correlations with the independent variables (%water, %oil, and S/C ratio) were significant ($P < 0.05$). This means that

quercetin MEs' viscosity increased as %W decreased and as %oil percent and S/C ratio increased. The presence of Tween 80, which has a high molecular weight, can increase viscosity values at high S/C ratios (21). Increased viscosity can enhance the preocular residence time and, thus, the amount of drug permeated into the cornea. The mean surface tension values of the ME samples were between 19.2 and 35.2 dynes/cm. The correlation between surface tension and the independent variables (%oil and S/C ratio) was significant. Thus, the surface tension of quercetin MEs increases as %oil decreases and as the S/C ratio increases.

The surface tension of tear fluids ranges from about 44 - 50 dyne/cm on the eye's surface. The administration of any ocular formulation could reduce surface tension at the eye, thereby resulting the disruption of external lipid layer of the tear film (34). The low surface tensions of MEs (19.2 - 35.2 dyne/cm) allow proper spreading on the corneal surface and make MEs suitable for mixing with the components of precorneal film. Therefore, the contact between drugs with the corneal epithelium layer is likely to be improved. Such findings confirm the previous report (35).

Following physical stability testing, we found that all tested MEs have appropriate properties concerning their droplet size uniformity, which remain stable after six months. There was no significant relationship between droplet size at the start of the research and droplet size six months later. Visual observations revealed no phase separation or precipitation.

The release profiles of quercetin MEs, the released percentage of the drug, and the kinetics of release in the chosen MEs are shown in Table 3. According to the drug release profile for ME-QU-8, which matched Higuchi's kinetic model, 98.06 percent of the drug was released within 24 hours of the experiment. Higuchi's model explains the release of drug amounts from MEs as the square root of time. ME-QU-8 had the lowest viscosity among all formulations, and it seems that lower viscosity causes a higher drug release percentage within 24 hours.

According to statistical findings, the quantity of medication released in 2 hours (R2h) did not have a significant relationship with any of the independent variables ($P > 0.05$), meanwhile, the quantity of drug released within 24 hours was shown to be substantially linked with the percentage of oil and the S/C ratio. Specifically, the amount of drug released from quercetin MEs in 24 hours increased as the S/C ratio decreased and as %Oil increased. In ocular drug delivery, the release of a drug from an ophthalmic preparation is very important as a first step in the therapeutic effects of the drug. ME systems have been categorized into various droplet structures and ordered or lamellar structures. In general, medications released from MEs may be divided into three phases: internal, exterior, and surfactant interphases. Two ideas have been proposed to explain drug release from ME carriers. The first model portrays drug diffusion as a rate-limiting stage of drug release, whereas the second model defines the interfacial barrier between the droplet and the surrounding region as a rate-determining step of drug release. The release of drugs from ME systems primarily depends on the average droplet size, oil and water phase ratio, and allocation of the drug in the ME phases.

Table 4 gives the enthalpy and cooling of the MEs' transition temperatures. According to the DSC results, water added to an ME carrier is either or free (bulk) or bound (interfacial) according to its state within the system (36). Based on the cooling curves of the ME samples, free water was produced at temperatures ranging from -11 to 0°C, whereas bound water was obtained at temperatures ranging from -28 to -18°C. Moreover, the melting transition temperatures of free and bound water ($Tm_1$ and $Tm_2$) were significantly correlated with the independent variables. Specifically, $Tm_1$ increased as %oil increased, and $Tm_2$ increased as %oil decreased. Moreover, independent variables appeared to influence the enthalpy of free water's exothermic peaks, significantly increasing with decreases in %oil and increases in %water and the S/C ratio.

The corneal permeability parameters of prepared quercetin MEs and their permeation percentages after 5 hours (%P5h) are shown in Table 3.

The amount of quercetin permeated a specified surface area the rabbit corneal membrane was plotted against time (h). The JSS of quercetin for ME-QU-8 in permeability studies was 58.88 $\mu g/cm^2h$, which is 8.8 times greater than the control (quercetin suspension, 0.2 percent). Statistical results showed that the correlation between $J_{ss}$ and the S/C ratio of ME samples was significant, as decreasing the S/C ratio caused $J_{ss}$ to increase. $T_{lag}$ and S/C ratio showed a substantial relationship, with an increase in S/C ratio leading to a large rise in $T_{lag}$. Apparent diffusivity coefficients ($D_{app}$) were not found to be significantly correlated with any of the independent variables. As a result, there was a substantial link between the $P_{app}$ parameter and the independent variable (S/C ratio), as a drop in the S/C ratio increased the Papp. The ME-QU-8 formulation had Dapp and Papp values of 0.009 $cm^2h^{-1}$ and 0.029 cm/h, respectively, which were greater than the control (quercetin suspension, 0.2 percent). The highest and lowest percentages of permeated drug after 5 hours (% P5h) were found at ME-QU-5 (16.1107%) and ME-QU-1 (0.6807%), respectively. In addition, there was no significant association between the percentage of penetrated drug after 5 hours (% P5h) and the independent variable. ME carriers strongly affected the flux in corneal permeation and permeation percentages of quercetin after 5 hours.ME structural compositions play an important role in corneal permeation. It has been shown that when hydrophilic and lipophilic drug molecules pass through

**Table 3.** The Percentage and Kinetics of Release of Selected Microemulsions and Permeability Parameters of Quercetin ME Formulations Through Rabbit Cornea (n = 3, Mean ± SD)

| Formulation Code | $J_{ss}$ ($\mu g/cm^2 h$) | $T_{Lag}$ (h) | $D_{app}$ ($cm^2/h$) | $P_{app}$ (cm/h) | $ER_{Flux}$ | $ER_D$ | $ER_P$ | %P (5h) | %Release (2 h) | % Release (24 h) | Kinetics of Release | $r^2$ |
|---|---|---|---|---|---|---|---|---|---|---|---|---|
| Control | 0.3 ± 0.001 | 3.4 ± 0.1 | 0.0005 ± 0.0001 | 0.018 ± 0.001 | _ | _ | _ | 0.2 ± 0.001 | - | - | - | - |
| ME-QU-1 | 34.241 ± 1.13 | 1.12 ± 1.141 | 0.0030 ± 0.003 | 0.017 ± 0.003 | 5.15 ± 0.92 | 6.31 ± 1.38 | 5.15 ± 0.93 | 0.6807 ± 0.076 | 9.627 ± 0.29 | 66.96 ± 0.53 | First | 0.9810 |
| ME-QU-2 | 27.761 ± 1.6 | 1.78 ± 0.09 | 0.0009 ± 0.00004 | 0.013 ± 0.005 | 4.17 ± 1.59 | 1.95 ± 0.1 | 4.18 ± 1.5 | 8.3043 ± 0.16 | 10.39 ± 1.09 | 31.017 ± 1.72 | Higuchi | 0.9978 |
| ME-QU-3 | 24.3 ± 1.2 | 0.92 ± 0.07 | 0.0018 ± 0.0001 | 0.012 ± 0.002 | 3.65 ± 0.7 | 3.79 ± 0.3 | 3.659 ± 0.78 | 13.864 ± 0.94 | 10.47 ± 0.12 | 44.16 ± 2.03 | Higuchi | 0.9387 |
| ME-QU-4 | 35.42 ± 1.34 | 1.9223 ± 1.3 | 0.00115 ± 0.0008 | 0.0177 ± 0.003 | 5.3296 ± 1.10 | 2.393 ± 1.7 | 5.3296 ± 1.1 | 6.6903 ± 0.203 | 24.03 ± 0.94 | 62.30 ± 2.62 | Higuchi | 0.8432 |
| ME-QU-5 | 37.76 ± 1.28 | 0.573 ± 0.3 | 0.0037 ± 0.002 | 0.018 ± 0.003 | 5.67 ± 0.9 | 7.85 ± 0.295 | 5.68 ± 0.94 | 16.1107 ± 0.37 | 15.56 ± 0.03 | 36.062 ± 3.37 | Higuchi | 0.8682 |
| ME-QU-6 | 44.6 ± 2.1 | 0.605 ± 0.06 | 0.0028 ± 0.0002 | 0.022 ± 0.001 | 6.8 ± 0.32 | 5.8 ± 0.6 | 6.708 ± 0.3 | 9.998 ± 2.35 | 7.678 ± 1.49 | 63.46 ± 3.92 | First | 0.9985 |
| ME-QU-7 | 41.6 ± 2.4 | 0.52 ± 0.3 | 0.0043 ± 0.003 | 0.020 ± 0.001 | 6.25 ± 0.36 | 9.16 ± 1.7 | ± 6.25 0.3 | 13.6276 ± 2.41 | 13.44 ± 0.66 | 97.89 ± 1.49 | zero | 0.9616 |
| ME-QU-8 | 58.88 ± 5.8 | 0.211 ± 0.08 | 0.009 ± 0.003 | 0.029 ± 0.003 | 8.8 ± 0.8 | 17.9 ± 2.3 | 8.8 ± 0.88 | 11.1841 ± 1.83 | 26.51 ± 1.39 | 98.06 ± 1.33 | Higuchi | 0.9869 |

**Table 4.** The Transition Temperature and Enthalpy of Quercetin Microemulsions (Mean ± SD, n = 3)

| Formulation | $Tm_1$, °C | ΔH1, mJ/mg | $Tm_2$, °C | ΔH2, mJ/mg |
|---|---|---|---|---|
| ME-QU-1 | -11 ± 0.1 | 2.55 ± 0.5 | -29 ± 1.1 | 34.23 ± 1 |
| ME-QU-2 | 0 | 0.75 ± 0.04 | -19 ± 0.12 | 36.14 ± 0.9 |
| ME-QU-3 | -7 ± 0.02 | 3.84 ± 0.01 | -18 ± 0.5 | 1.18 ± 0.4 |
| ME-QU-4 | -8 ± 0.01 | 4.39 ± 0.02 | -18 ± 0.1 | 2.30 ± 0.7 |
| ME-QU-5 | -9 ± 0.01 | 2.54 ± 0.01 | -18 ± 0.1 | 2.57 ± 0.1 |
| ME-QU-6 | -8 ± 0.03 | 1.22 ± 0.05 | -18 ± 0.6 | 1.69 ± 0.12 |
| ME-QU-7 | 0 | 0.63 ± 0.2 | -31 ± 1.1 | 28.89 ± 0.4 |
| ME-QU-8 | 0 | 0.1 ± 0.001 | -28 ± 0.9 | 38.72 ± 0.5 |

the cornea, the oleic acid concentration of MEs is altered (37). Another previous study describes changes in the microstructure of bio-barriers caused by oleic acid. Specifically, oleic acid rearranges lipid bilayers to make diffusion routes for drug molecules to travel along (38).

Surfactants are another ingredient in ME systems that enhance drug penetration, thereby allowing more of an administered drug to reach its target. Taniguchi et al. reported that Tween 80 enhanced corneal permeability to hydrophobic drugs (39). In other cases—specifically, if the goal is to improve permeability—surfactant materials can be introduced to change the membrane's properties. Such changes are instigated as the protective properties of tear film and mucin are counteracted. As a result, the whole epithelial layer is disrupted as the connections between cell membranes are weakened or otherwise modified to foster permeability (40).

The Transcutol P contained within quercetin MEs improves drugs' corneal permeability because it alters the corneal barrier's functioning. In a previous study, Kuar and Smitha observed that some outer cell membranes comprised a phospholipid bilayer, along with protein-molecule-containing lipid membrane, which was encompassed by corneal epithelial cells (41). The micelles produced by Transcutol P improve drugs' transcorneal permeation by reducing the level of phospholipids on the membranes of epithelial cells. One drawback is that lipophilic molecule movement can be reduced when Transcutol P is utilized, as its use can cause hydration barriers to form (42).

The results obtained for the thermograms indicate that rabbit corneas have two transition phases at temperatures of 64°C and 146°C. These phase transition temperatures were thoroughly shifted for corneas in contact with quercetin ME formulations to temperatures lower than 61°C and 124°C, showing negative shifts in phase transition temperatures of about 3°C and 24°C, respectively. On the other hand, phase transition enthalpies significantly decreased. Therefore, it seems that all quercetin ME formulations affected the rabbit cornea structure and change phase transition temperatures. These results suggest that quercetin-loaded MEs interacted with cornea structures

and increased the level of quercetin corneal permeation (43).

## 5. Conclusions

In this study, various formulations of quercetin ME were prepared by a factorial design method for ocular delivery. The results indicate that all of the selected quercetin MEs have acceptable physicochemical properties—especially droplet size, release behavior, corneal permeability, and stability for ocular use. ME samples had an average viscosity of 115 - 361 cps, a pH range of 5.22 - 6.20, and a droplet size range of 5.31-26.07 nm. The MEs had mean surface tensions of 19.2 and 35.2 dynes/cm, respectively. The correlations between surface tension, oil percentage, and S/C ratio in formulations were significant. The low surface tensions of MEs allow for proper spreading on the corneal surface. The quantity of drug released in vitro in 24 hours in MEs was substantially associated with the S/C ratio and oil percentage, with the amount of drug released increasing as the S/C ratio decreased and the oil percentage grew. Within the first 24 hours of the trial, 98.06 percent of quercetin was released from ME-QU-8, according to the drug release curve. According to the Higuchi kinetic model, this mixture contained 50% oleic acid and Transcutol P, 40% Smix (a 1:1 mixture of Tween 80 and Span 20-propylene glycol), and 10% water. In the permeability experiment, the Jss of quercetin for ME-QU-8 was 58.88 $\mu$g/cm$^2$h, which was 8.8 times greater than the control. Furthermore, there was a substantial link between $J_{ss}$ and the S/C ratio, with reductions in the S/C ratio causing increases in $J_{ss}$. The ME-QU-8 formulations had Dapp and Papp values of 0.009 cm$^2$/h and 0.029 cm/h, which were higher than the control. The ME-QU-5 had the greatest percentage of drug permeation after 5 hours (% P5h), at 16.1107 percent. This combination included 5% oleic acid and Transcutol P, 85% Smix (a 1:1 mixture of Tween 80 and Span 20-propylene glycol), and 10% water. There was no significant association between %P5h and the independent factors. Quercetin ME formulations affected the rabbit cornea structure and changed the phase transition temperatures. These results show that quercetin-loaded MEs interacted with the cornea structure and increased the level of quercetin corneal permeation.

## Footnotes

**Authors' Contribution:** It was not declared by the authors.

**Conflict of Interests:** Salimi is one of the reviewers of this journal. The authors hereby certify that they have no conflict of interest.

**Data Reproducibility:** No new data were created or analyzed in this study.

**Ethical Approval:** The current experiment was approved by the Ahvaz Jundishapur University of Medical Sciences' animal ethics committee (permission number IR.AJUMS.ABHC.REC.1397.020). Link: ethics.research.ac.ir/ProposalCertificateEn.php?id=15669.

**Funding/Support:** This study was supported in part by grant (33012456) Ahvaz Jundishapur University of Medical Sciences provided funding for the research. (Webpage of the grant number: behsan.ajums.ac.ir/webdocument/load.action?webdocument_code=1000&masterCode=33012456)

## References

1. Alami-Milani M, Zakeri-Milani P, Valizadeh H, Salehi R, Salatin S, Naderinia A, et al. Novel Pentablock Copolymers as Thermosensitive Self-Assembling Micelles for Ocular Drug Delivery. *Adv Pharm Bull*. 2017;**7**(1):11–20. doi: 10.15171/apb.2017.003. [PubMed: 28507933]. [PubMed Central: PMC5426723].
2. Shen J, Wang Y, Ping Q, Xiao Y, Huang X. Mucoadhesive effect of thiolated PEG stearate and its modified NLC for ocular drug delivery. *J Control Release*. 2009;**137**(3):217–23. doi: 10.1016/j.jconrel.2009.04.021. [PubMed: 19393270].
3. Araujo J, Gonzalez E, Egea MA, Garcia ML, Souto EB. Nanomedicines for ocular NSAIDs: safety on drug delivery. *Nanomedicine*. 2009;**5**(4):394–401. doi: 10.1016/j.nano.2009.02.003. [PubMed: 19341814].
4. Zhang W, Prausnitz MR, Edwards A. Model of transient drug diffusion across cornea. *J Control Release*. 2004;**99**(2):241–58. doi: 10.1016/j.jconrel.2004.07.001. [PubMed: 15380634].
5. Gao XC, Qi HP, Bai JH, Huang L, Cui H. Effects of oleic acid on the corneal permeability of compounds and evaluation of its ocular irritation of rabbit eyes. *Curr Eye Res*. 2014;**39**(12):1161–8. doi: 10.3109/02713683.2014.904361. [PubMed: 24749683].
6. Bhattacharjee A, Das PJ, Adhikari P, Marbaniang D, Pal P, Ray S, et al. Novel drug delivery systems for ocular therapy: With special reference to liposomal ocular delivery. *Eur J Ophthalmol*. 2019;**29**(1):113–26. doi: 10.1177/1120672118769776. [PubMed: 29756507].
7. Sahoo SK, Dilnawaz F, Krishnakumar S. Nanotechnology in ocular drug delivery. *Drug Discov Today*. 2008;**13**(3-4):144–51. doi: 10.1016/j.drudis.2007.10.021. [PubMed: 18275912].
8. Diebold Y, Calonge M. Applications of nanoparticles in ophthalmology. *Prog Retin Eye Res*. 2010;**29**(6):596–609. doi: 10.1016/j.preteyeres.2010.08.002. [PubMed: 20826225].
9. Omerović N, Vranić E. Application of nanoparticles in ocular drug delivery systems. *Health Technol*. 2019;**10**(1):61–78. doi: 10.1007/s12553-019-00381-w.
10. Lamson DW, Brignall MS. Antioxidants and cancer, part 3: quercetin. *Altern Med Rev*. 2000;**5**(3):196–208. [PubMed: 10869101].
11. Shoham A, Hadziahmetovic M, Dunaief JL, Mydlarski MB, Schipper HM. Oxidative stress in diseases of the human cornea. *Free Radic Biol Med*. 2008;**45**(8):1047–55. doi: 10.1016/j.freeradbiomed.2008.07.021. [PubMed: 18718524].
12. Russo M, Spagnuolo C, Tedesco I, Bilotto S, Russo GL. The flavonoid quercetin in disease prevention and therapy: facts and fancies. *Biochem Pharmacol*. 2012;**83**(1):6–15. doi: 10.1016/j.bcp.2011.08.010. [PubMed: 21856292].
13. Carini JP, Klamt F, Bassani VL. Flavonoids from Achyrocline satureioides: promising biomolecules for anticancer therapy. *RSC Adv*. 2014;**4**(7):3131–44. doi: 10.1039/c3ra43627f.

14. Stefek M, Karasu C. Eye lens in aging and diabetes: effect of quercetin. *Rejuvenation Res*. 2011;**14**(5):525–34. doi: 10.1089/rej.2011.1170. [PubMed: 21978083].
15. McKay TB, Karamichos D. Quercetin and the ocular surface: What we know and where we are going. *Exp Biol Med (Maywood)*. 2017;**242**(6):565–72. doi: 10.1177/1535370216685187. [PubMed: 28056553]. [PubMed Central: PMC5685256].
16. Romero J, Marak GJ, Rao NA. Pharmacologic modulation of acute ocular inflammation with quercetin. *Ophthalmic Res*. 1989;**21**(2):112–7. doi: 10.1159/000266788. [PubMed: 2786615].
17. Ustundag Okur N, Caglar ES, Siafaka PI. Novel Ocular Drug Delivery Systems: An Update on Microemulsions. *J Ocul Pharmacol Ther*. 2020;**36**(6):342–54. doi: 10.1089/jop.2019.0135. [PubMed: 32255728].
18. Salimi A. Preparation and evaluation of celecoxib nanoemulsion for ocular drug delivery. *Asian J Pharm*. 2017;**11**(3). doi: 10.22377/ajp.v11i03.1457.
19. Vandamme TF. Microemulsions as ocular drug delivery systems: recent developments and future challenges. *Prog Retin Eye Res*. 2002;**21**(1):15–34. doi: 10.1016/s1350-9462(01)00017-9.
20. Lawrence M, Rees GD. Microemulsion-based media as novel drug delivery systems. *Adv Drug Deliv Rev*. 2000;**45**(1):89–121. doi: 10.1016/s0169-409x(00)00103-4.
21. Kajbafvala A, Salabat A, Salimi A. Formulation, characterization, and in vitro/ex vivo evaluation of quercetin-loaded microemulsion for topical application. *Pharm Dev Technol*. 2018;**23**(8):741–50. doi: 10.1080/10837450.2016.1263995. [PubMed: 27871215].
22. Mohammad Soleymani S, Salimi A. Enhancement of Dermal Delivery of Finasteride Using Microemulsion Systems. *Adv Pharm Bull*. 2019;**9**(4):584–92. doi: 10.15171/apb.2019.067. [PubMed: 31857962]. [PubMed Central: PMC6912190].
23. Hegde RR, Verma A, Ghosh A. Microemulsion: new insights into the ocular drug delivery. *ISRN Pharm*. 2013;**2013**:826798. doi: 10.1155/2013/826798. [PubMed: 23936681]. [PubMed Central: PMC3712243].
24. Moghimipour E, Salimi A, Changizi S. Preparation and Microstructural Characterization of Griseofulvin Microemulsions Using Different Experimental Methods: SAXS and DSC. *Adv Pharm Bull*. 2017;**7**(2):281–9. doi: 10.15171/apb.2017.034. [PubMed: 28761831]. [PubMed Central: PMC5527243].
25. Shah RR, Magdum CS, Patil SS, Niakwade NS. Preparation and evaluation of aceclofenac topical microemulsion. *Iran J Pharm Sci*. 2010;**9**(1):5–11. doi: 10.22037/IJPR.2010.829.
26. Zhang X, Sun X, Li J, Zhang X, Gong T, Zhang Z. Lipid nanoemulsions loaded with doxorubicin-oleic acid ionic complex: characterization, in vitro and in vivo studies. *Die Pharmazie*. 2011;**66**(7):496–505. doi: 10.1691/ph.2011.0379.
27. Salimi A, Zadeh BSM, Moghimipour E. Preparation and characterization of cyanocobalamin (Vit B12) microemulsion properties and structure for topical and transdermal application. *Iran J Basic Med Sci*. 2013;**16**(7):865–872.
28. Mergler S, Pleyer U. The human corneal endothelium: new insights into electrophysiology and ion channels. *Prog Retin Eye Res*. 2007;**26**(4):359–78. doi: 10.1016/j.preteyeres.2007.02.001. [PubMed: 17446115].
29. Greenbaum A, Hasany SM, Rootman D. Optisol vs Dexsol as storage media for preservation of human corneal epithelium. *Eye (Lond)*. 2004;**18**(5):519–24. doi: 10.1038/sj.eye.6700693. [PubMed: 15131685].
30. Abdelkader H, Ismail S, Kamal A, Alany RG. Design and evaluation of controlled-release niosomes and discomes for naltrexone hydrochloride ocular delivery. *J Pharm Sci*. 2011;**100**(5):1833–46. doi: 10.1002/jps.22422. [PubMed: 21246556].
31. Salimi A, Panahi-Bazaz M, Panahi-Bazaz E. A Novel Microemulsion System for Ocular Delivery of Azithromycin: Design, Characterization and Ex-Vivo Rabbit Corneal Permeability. *Jundishapur J Nat Pharm Prod*. 2017;**12**(2). doi: 10.5812/jjnpp.13938.
32. Monti D, Chetoni P, Burgalassi S, Najarro M, Saettone MF. Increased corneal hydration induced by potential ocular penetration enhancers: assessment by differential scanning calorimetry (DSC) and by desiccation. *Int J Pharm*. 2002;**232**(1-2):139–47. doi: 10.1016/s0378-5173(01)00907-3. [PubMed: 11790497].
33. Wang H, Li Q, Reyes S, Zhang J, Xie L, Melendez V, et al. Formulation and particle size reduction improve bioavailability of poorly water-soluble compounds with antimalarial activity. *Malar Res Treat*. 2013;**2013**:769234. doi: 10.1155/2013/769234. [PubMed: 23766925]. [PubMed Central: PMC3666196].
34. Tiffany JM, Winter N, Bliss G. Tear film stability and tear surface tension. *Curr Eye Res*. 1989;**8**(5):507–15. doi: 10.3109/02713688909000031. [PubMed: 2736956].
35. Nair R, Chakrapani M, Kaza R. Preparation and Evaluation of Vancomycin Microemulsion for Ocular Drug Delivery. *Drug Deliv Lett*. 2012;**2**(1):26–34. doi: 10.2174/2210303111202010026.
36. Garti N, Aserin A, Tiunova I, Fanun M. A DSC study of water behavior in water-in-oil microemulsions stabilized by sucrose esters and butanol. *Colloids Surf*. 2000;**170**(1):1–18. doi: 10.1016/s0927-7757(00)00486-6.
37. Moreira TS, de Sousa VP, Pierre MB. Influence of oleic acid on the rheology and in vitro release of lumiracoxib from poloxamer gels. *J Pharm Pharm Sci*. 2010;**13**(2):286–302. doi: 10.18433/j34880. [PubMed: 20816013].
38. Notman R, Noro MG, Anwar J. Interaction of oleic acid with dipalmitoylphosphatidylcholine (DPPC) bilayers simulated by molecular dynamics. *J Phys Chem B*. 2007;**111**(44):12748–55. doi: 10.1021/jp0723564. [PubMed: 17939702].
39. Taniguchi K, Itakura K, Morisaki K, Hayashi S. Effects of Tween 80 and liposomes on the corneal permeability of anti-inflammatory steroids. *J Pharmacobiodyn*. 1988;**11**(10):685–93. doi: 10.1248/bpb1978.11.685. [PubMed: 3221301].
40. Moiseev RV, Morrison PWJ, Steele F, Khutoryanskiy VV. Penetration Enhancers in Ocular Drug Delivery. *Pharmaceutics*. 2019;**11**(7). doi: 10.3390/pharmaceutics11070321. [PubMed: 31324063]. [PubMed Central: PMC6681039].
41. Kaur IP, Smitha R. Penetration enhancers and ocular bioadhesives: two new avenues for ophthalmic drug delivery. *Drug Dev Ind Pharm*. 2002;**28**(4):353–69. doi: 10.1081/ddc-120002997. [PubMed: 12056529].
42. Tang-Liu DD, Richman JB, Weinkam RJ, Takruri H. Effects of four penetration enhancers on corneal permeability of drugs in vitro. *J Pharm Sci*. 1994;**83**(1):85–90. doi: 10.1002/jps.2600830120. [PubMed: 8138917].
43. Taka E, Karavasili C, Bouropoulos N, Moschakis T, Andreadis DDD, Zacharis CKK, et al. Ocular co-Delivery of Timolol and Brimonidine from a Self-Assembling Peptide Hydrogel for the Treatment of Glaucoma: In Vitro and Ex Vivo Evaluation. *Pharmaceuticals (Basel)*. 2020;**13**(6). doi: 10.3390/ph13060126. [PubMed: 32575910]. [PubMed Central: PMC7344471].